Improved Transient Performance by Lyapunov-based Integrator Reset of PI Thruster Control in Extreme Seas

Jostein Bakkeheim*, Øyvind N. Smogeli†, Tor A. Johansen* and Asgeir J. Sørensen†
*Department of Engineering Cybernetics, Norwegian University of Science and Technology, Trondheim, Norway.
†Department of Marine Technology, Norwegian University of Science and Technology, Trondheim, Norway.

***Abstract*— PI controllers are often tuned such that the overall performance is a trade-off between performance in steady state and transient regimes. By introducing reset of the integrator value in these controllers, the performance in transient regimes may be increased without influencing the performance in steady state. An advantage of this strategy is that it can be integrated into an already existing controller as a separate module. This will only affect the performance in the transient regimes, by speeding up the controller response only when large control errors are measured. We will in this paper show how integrator reset can be used for anti-spin in local thruster speed control on ships with electric propulsion. Transient regimes arise when the ship is in extreme seas, where ventilation and in-and-out of water effects may give rise to loss in propeller thrust. In this paper, a Lyapunov function is used to decide when a reset of the integrator value is appropriate. The method is illustrated with experimental results.**

I. Introduction

Electrically driven thrusters are becoming the standard in advanced ship propulsion for offshore vessels, cruise vessels, navy ships and some advanced tankers. In these systems, thrusters are electrically driven taking the power from power buses, where the power is supplied by generators driven by diesel engines or gas turbines. The control hierarchy consists of a high-level controller giving commands to a thrust allocation scheme, which in turn gives commanded thrust set-points to the different local thruster controllers (LTC), see [1]. Examples of high-level controllers are dynamic positioning (DP) systems, joysticks and autopilots. In many cases the LTC is a conventional PI-controller, controlling the propeller shaft speed. The PI-controller may be tuned such that the performance is acceptable in both steady-state and transient regimes. The faster the PI-controller is tuned, the better the controller will perform in transient regimes. This will in turn increase the sensitivity to noise and increase variations in torque, power and mechanical load, and hence decrease the performance while in steady-state.

In normal operation, there may be no need for high transient performance. When the ship is in extreme seas, however, the propeller may start to spin due to ventilation and in-and-out-of water effects. This, in turn, may lead to wear and tear of the ship's propulsion equipment and undesired transients on the power bus that may increase the risk of blackouts due to overloading of the generator sets, see [2].

To handle these phenomena, an anti-spin controller is developed in [3], which utilizes an estimate of the torque loss to detect ventilation incidents. The anti-spin controller in [3] is based on a combined power/torque controller which in order takes control of the propeller shaft speed. A similar approach is considered here, but instead the anti-spin controller is based on a standard shaft speed PI-controller, where the integrator value may be reset if appropriate. The torque loss observer in [3] is here utilized for online calculation of the Lyapunov function origin (equilibrium point), hence the Lyapunov function value may jump to a higher value when the propeller starts or stops ventilating. A multiple model Lyapunov algorithm decides when to take integrator reset actions, selecting the integrator value which gives the greatest drop in the Lyapunov function value. This approach may also includes the possibility of hard constraints, such as power limitations, propeller speed limitations etc. The advantage of such a reset approach is that the only alteration from prevailing installations are more or less restricted to software updates.

II. Local thruster controller

An illustration of a local thruster shaft speed control system is given in Figure 1. From the high-level control module, the desired propeller thrust T_d is given as an input to the controller. Further, a direct mapping transforms this into the desired shaft speed ω_d. This is in turn fed into a set-point mapping, which may limit the value of the desired shaft speed to cope with possible events of ventilation, see [3] for more details. The main idea pursued in this paper is that the integrator in the PI-controller may be reset to a different value to make the thruster approach its new steady state value faster.

Locally, one may look at this controller as an ordinary PI-controller, which is in addition able to reset the integrator value. With reference to Figure 1, the different blocks; thruster model, PI-controller, thrust to propeller speed mapping, set-point mapping, integrator resetting, propeller load torque observer and ventilation detection are considered in the following.

A. Thruster model

The rotational dynamics are described as in [4] p. 473 by a first-order dynamic model for the propeller and shaft:

$$J\dot{\omega} = Q_c - Q_p(\frac{h}{R}, \omega) - K_\omega \omega \tag{1}$$

where Q_c is commanded torque, J is the rotational inertia of the propeller (including hydrodynamic added mass, shaft, gears and motor), K_ω is a linear friction coefficient, ω is the angular speed of the propeller, and Q_p is the propeller load torque. The load torque Q_p is here modelled as:

$$Q_p(\frac{h}{R}, \omega) = Q_n(\omega)\beta_Q(\frac{h}{R}, \frac{\omega}{\omega_{max}}) \tag{2}$$

where h/R is the relative submergence of the propeller, with R being the radius of the propeller, and h the shaft submergence. The nominal torque Q_n is given as:

$$Q_n(\omega) = \Phi sgn(\omega)\omega^2 \tag{3}$$

where $\Phi = (K_{Q0}\rho D^5)/(4\pi^2)$, D is the propeller diameter, and ρ is the density of water. K_{Q0} is the nominal torque

* E-mail: {josteib, taj}@itk.ntnu.no
† E-mail: {oyvind.smogeli, asgeir.sorensen}@ntnu.no

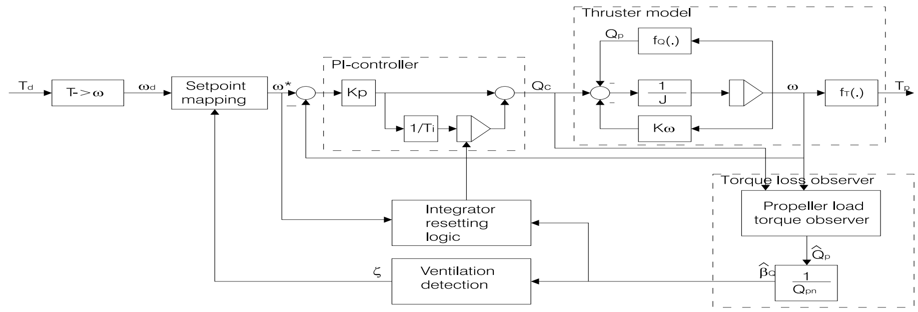

Fig. 1. Local thruster control system.

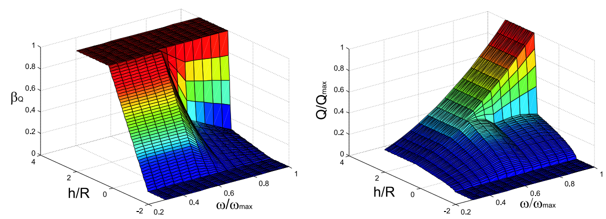

(a) Ventilation loss function β_Q. (b) Propeller load torque.

Fig. 2. Ventilation loss and propeller load torque as functions of relative submergence h/R and relative shaft speed ω/ω_{max}.

coefficient commonly used for DP and low speed manoeuvering operations, when the advance speed V_a is low. For transit operations with higher V_a, other models for K_Q can be established. β_Q in (2) expresses the torque loss, which is the ratio of actual to nominal torque, where ω_{max} is a chosen maximum speed of the propeller. Figure 2(a) shows a typical shape of this torque loss coefficient, see [5] for more details.

B. *PI-controller*

Given a PI-controller:

$$Q_c = K_p\left(\omega^* - \omega\right) + z \tag{4}$$

where $K_p > 0$ is the proportional gain and the integrator state is:

$$\dot{z} = K_I\left(\omega^* - \omega\right) \tag{5}$$

with $K_I = K_p/T_i$ and $T_i > 0$ the integral time constant. The complete closed loop system becomes:

$$\begin{aligned} \dot{\omega} &= \frac{1}{J}\left(-K_p\omega + K_p\omega^* - K_\omega\omega - Q_p(\frac{h}{R},\omega) + z\right) \quad (6)\\ \dot{z} &= -K_I\omega + K_I\omega^* \end{aligned}$$

with $K_\omega, J > 0$ system constants.

Assuming h/R and ω^* being constant, we also obtain steady state values for z, i.e.:

$$z^* = K_\omega\omega^* + Q_p(\frac{h}{R},\omega^*) \tag{7}$$

Based on the definition of the error variables $\tilde{\omega} = \omega^* - \omega$ and $\tilde{z} = z^* - z$, we have the following error dynamics:

$$\begin{aligned} \dot{\tilde{\omega}} &= \frac{1}{J}\left(\tilde{z} - (K_p + K_\omega)\,\tilde{\omega} + \left(Q_p(\frac{h}{R},\omega) - Q_p(\frac{h}{R},\omega^*)\right)\right) \quad (8)\\ \dot{\tilde{z}} &= -K_I\tilde{\omega} \end{aligned}$$

Further defining $\tilde{x} = [\tilde{\omega},\ \tilde{z}]^T$, the control error may be written in compact form:

$$\dot{\tilde{x}} = A\tilde{x} + \frac{1}{J}F(\tilde{x},\frac{h}{R},\omega^*) \tag{9}$$

where

$$A = \begin{bmatrix} -\frac{1}{J}\left(K_\omega + K_p - a\right) & \frac{1}{J} \\ -K_I & 0 \end{bmatrix} \tag{10}$$

$$F(\tilde{x},\frac{h}{R},\omega^*) = \begin{bmatrix} f\left(\frac{h}{R},\omega^*,\tilde{\omega}\right) \\ 0 \end{bmatrix} \tag{11}$$

$$f(\frac{h}{R},\omega^*,\tilde{\omega}) = Q_p(\frac{h}{R},\omega) - Q_p(\frac{h}{R},\omega^*) - a\tilde{\omega} \tag{12}$$

The linear part $a\tilde{\omega}$ is subtracted from the nonlinearity in (8), leaving $F(\tilde{x},\frac{h}{R},\omega^*)$ as the remaining nonlinear part in (9). This is done in order to incorporate a linear approximation of the nonlinear part of the system as accurately as possible. The nonlinear system may then be approximated by a linear system. We search for a Lyapunov function as for the linear systems, and analyze the effects of the nonlinearity later.

We know that for A in (9) being Hurwitz, there exists a solution $P^T = P > 0$ of the Lyapunov equation:

$$A^T P + PA = -Q \tag{13}$$

where $Q^T = Q > 0$ and in general

$$P = \begin{bmatrix} p_{11} & p_{12} \\ p_{12} & p_{22} \end{bmatrix} \tag{14}$$

The following choice of Lyapunov candidate:

$$V(\tilde{x}) = \tilde{x}^T P\tilde{x} \tag{15}$$

will prove stability of the closed loop system.

Proposition 1: Assume ω^* and h/R constant, and suppose K_I and K_p are chosen such that A in (9) is Hurwitz and $P^T = P > 0$ is a solution to the Lyapunov equation (13), where $Q = \mathrm{diag}(q_{11}, q_{22}) > 0$. Further, if there exists an α such that the graph of $f(\frac{h}{R},\omega^*,\tilde{\omega})$ in (11) belongs to the sector $[-\alpha,\alpha]$, $\forall\ \tilde{\omega} \in \mathbb{R}$, and there exist $\mu_1 > 0$ and $\mu_2 > 0$ such that

$$q_{11} - \frac{1}{J}(\mu_1 + \mu_2)\alpha^2 - \frac{1}{J\mu_1}(p_{11})^2 > 0 \tag{16}$$

$$q_{22} - \frac{1}{J\mu_2}(p_{12})^2 > 0 \tag{17}$$

holds, then the origin $\tilde{x} = 0$ is a globally exponentially stable (GES) equilibrium point of (9).

Proof: The time derivative of (15) along the trajectories of the nonlinear system (9) is:

$$\dot{V}(\tilde{x}) = -\tilde{x}^T Q\tilde{x} + \frac{2}{J}\tilde{x}^T PF(\tilde{x}, \frac{h}{R}, \omega^*) \tag{18}$$

The two terms in (18) are:

$$-\tilde{x}^T Q\tilde{x} = -q_{11}\tilde{\omega}^2 - q_{22}\tilde{z}^2 - 2q_{12}\tilde{\omega}\tilde{z} \tag{19}$$

$$\begin{aligned}\frac{2}{J}\tilde{x}^T PF(\tilde{x}, \frac{h}{R}, \omega^*) &= \frac{2}{J}p_{11}\tilde{\omega}f(\frac{h}{R}, \omega^*, \tilde{\omega}) \\ &+ \frac{2}{J}p_{12}\tilde{z}f(\frac{h}{R}, \omega^*, \tilde{\omega})\end{aligned} \tag{20}$$

Using Young's inequality, $2xy \leq \frac{1}{\mu}x^2 + \mu y^2, \quad \forall \mu > 0$, on the second term of (20), we obtain:

$$\begin{aligned}\frac{2}{J}\tilde{x}^T PF(\tilde{x}, \frac{h}{R}, \omega^*) \leq \frac{1}{J\mu_1}(p_{11}\tilde{\omega})^2 + \frac{1}{J}\mu_1 f^2(\frac{h}{R}, \omega^*, \tilde{\omega}) \\ + \frac{1}{J\mu_2}(p_{12}\tilde{z})^2 + \frac{1}{J}\mu_2 f^2(\frac{h}{R}, \omega^*, \tilde{\omega})\end{aligned} \tag{21}$$

Since Q is diagonal and $f(\frac{h}{R}, \omega^*, \tilde{\omega})$ belongs to the sector $[-\alpha, \alpha]$, i.e. $f^2(\frac{h}{R}, \omega^*, \tilde{\omega}) \leq (\alpha\tilde{\omega})^2$, $\forall\tilde{\omega}$ for constant ω^* and $\frac{h}{R}$, we obtain:

$$\begin{aligned}\dot{V}(\tilde{x}) \leq &-\left(q_{11} - \frac{1}{J}(\mu_1 + \mu_2)\alpha^2 - \frac{1}{J\mu_1}(p_{11})^2\right)\tilde{\omega}^2 \\ &-\left(q_{22} - \frac{1}{J\mu_2}(p_{12})^2\right)\tilde{z}^2 = -W(\tilde{x})\end{aligned} \tag{22}$$

From (16)-(17), the function $W(\tilde{x})$ is positive definite, hence GES follows from Thm 4.1 in [6]. ∎

Note that for a sudden change in the loss factor β_Q, the Lyapunov function value will make a positive jump due to its new equilibrium point.

C. Thrust to propeller speed mapping

For fixed pitch propellers, the industrial standard is shaft speed control based on a static mapping from desired thrust T_d to desired shaft speed ω_d. We use the following mapping:

$$\omega_d = 2\pi\text{sgn}(T_d)\sqrt{\left|\frac{T_d}{K_{T0}\rho D^4}\right|} \tag{23}$$

Note that in this mapping, the nominal thrust coefficient for $V_a = 0$, K_{T0}, is used. In transit where $V_a \neq 0$, an alternative thrust coefficient $K_T(V_a)$ could be used.

D. Integrator resetting

Integrator reset may improve performance in transient regimes, when the equilibrium suddenly changes due to ventilation, without influencing performance in steady-state. Stability should be ensured even when these reset incidents occur. A reset criterion can be stated with the help of the already obtained Lyapunov function.

To maintain stability when the integrator is reset, one may perform a reset only when this leads to a negative jump in the Lyapunov function. Changes in value of the Lyapunov function (15) due to reset of the integrator, is stated in the following lemma.

Lemma 1: A reset of the integrator value $z(t^+)$ to z_i, where t^+ denotes an infinitely small time increment of t, of system (9) leads to a jump in the Lyapunov function (15) as follows:

$$\Delta V_i(t) = p_{22}\left(\tilde{z}_i^2 - \tilde{z}^2(t)\right) + 2p_{12}\tilde{\omega}(t)\left(\tilde{z}_i - \tilde{z}(t)\right) \tag{24}$$

where $\tilde{z}_i = z^* - z_i$.

Proof: Let $\tilde{\omega}_i = \omega^* - \omega_i$ and $\tilde{x}_i = [\tilde{\omega}_i, \tilde{z}_i]^T$. The jump in the Lyapunov function is calculated as follows:

$$\begin{aligned}\Delta V_i(t) = V(\tilde{x}_i) - V(\tilde{x}(t)) &= \tilde{x}_i^T P\tilde{x}_i - \tilde{x}^T(t)P\tilde{x}(t) \\ &= p_{11}\tilde{\omega}_i^2 + p_{22}\tilde{z}_i^2 + 2p_{12}\tilde{\omega}_i\tilde{z}_i \\ &- p_{11}\tilde{\omega}^2(t) - p_{22}\tilde{z}^2(t) - 2p_{12}\tilde{\omega}(t)\tilde{z}(t) \\ &= p_{22}\left(\tilde{z}_i^2 - \tilde{z}^2(t)\right) + 2p_{12}\tilde{\omega}(t)\left(\tilde{z}_i - \tilde{z}(t)\right)\end{aligned} \tag{25}$$

where the fact that $\tilde{\omega}_i = \tilde{\omega}(t)$, due to the continuity of solutions of ordinary differential equations, has been used. ∎

We assume a finite set of integrator reset candidates, $\mathcal{H} = \{z_1, \ldots, z_n\}$. The following result states stability when the integrator is reset.

Theorem 1: Given a closed-loop system with PI-controller as in (9). Assume that $V(t)$ in (15) is a Lyapunov function that proves the equilibrium point of the nonlinear system in (9) to be GES. Further assume that $\Delta V_i(t)$ denotes the jump in the Lyapunov function value if the integrator of the PI-controller in (9) is reset to a different value $z_i \in \mathcal{H}$. Then if z is reset to the value z_i only if $\Delta V_i(t) < 0$, the equilibrium point of the nonlinear system in (9) is GES.

Proof: The reader is referred to [7], where the switching system is proved to be stable in sense of Lyapunov if $\Delta V_i(t) < 0$. Further, the condition $\Delta V_i(t) < 0$ leads to a negative jump in the Lyapunov function, which also leads to $\dot{V}(\tilde{x}) \leq -W(\tilde{x})$ in (22), hence GES follows. ∎

Remark 1: Assume the choice of Q in (13) is done in such a way that the Lyapunov function is an appropriate measure of remaining transient trajectory. Then, in addition to the overall stability being preserved with resetting, there will be a transient performance improvement if the system is reset.

E. Propeller load torque observer

Based on the rotational dynamics (1), the observer equations for the estimated propeller load torque $\hat{Q}_p$ presented in [8] are written as:

$$\begin{aligned}\dot{\hat{\omega}} &= \frac{1}{J}(-\hat{Q}_p - K_\omega\hat{\omega} + Q_c) + k_1(y - \hat{y}), \\ \dot{\hat{Q}}_p &= -k_2(y - \hat{y}),\end{aligned} \tag{26}$$

where the propeller load torque Q_p has been modelled as $\dot{Q}_p = 0$, and the shaft speed ω is taken as the measured output y (and hence $\hat{y} = \hat{\omega}$). The equilibrium point of the observer error dynamics is globally exponentially stable (GES) in the case of a constant load torque if the observer gains k_1 and k_2 are chosen according to [8]:

$$k_1 > -K_\omega/J, \quad k_2 < 0. \tag{27}$$

An estimate of the torque loss factor β_Q may be calculated based on the estimated propeller load torque $\hat{Q}_p$ from (26) and an estimated expected nominal load torque $\hat{Q}_n$. $\hat{Q}_n$ is given from (3) by feedback from the propeller shaft speed ω as:

$$\hat{Q}_n(\omega) = \Phi sgn(\omega)\omega^2. \tag{28}$$

The estimated torque loss with respect to the nominal torque expected from the measured shaft speed is then:

$$\hat{\beta}_Q = \alpha_b(\omega) + (1 - \alpha_b(\omega))\frac{\hat{Q}_p}{\hat{Q}_n}. \tag{29}$$

$\alpha_b(\omega)$ is a weighting function of the type:

$$\alpha_b(y) = e^{-k|py|^r} \quad \text{for} \quad y \in \mathbb{R}, \tag{30}$$

where k, p and r are positive tuning gains. The weighting function is needed because the estimate otherwise would be singular for zero shaft speed [8].

F. Ventilation detection

The estimated loss factor $\hat{\beta}_Q$ may be subject to some fluctuations during the period of ventilation. Instead of using this estimate directly as a measure of whether the propeller is ventilating or not, a translation of this value into a discrete value ζ may be appropriate, as in [3]. For a single ventilation incident, ζ will have the following evolution:

$$\begin{array}{ll} \hat{\beta}_Q \geq \beta_{v,on} \Rightarrow \zeta = 0 & \text{(no ventilation)} \\ \hat{\beta}_Q < \beta_{v,on} \Rightarrow \zeta = 1 & \text{(ventilation)} \\ \hat{\beta}_Q \geq \beta_{v,off} \Rightarrow \zeta = 0 & \text{(no ventilation)} \end{array} \tag{31}$$

G. Effects of not knowing the loss value

Because the loss factor β_Q is unknown, the steady state value z^* in (7) is estimated:

$$\hat{z}^* = K_\omega \omega^* + \Phi sgn(\omega^*)\omega^{*2}\hat{\beta}_Q \tag{32}$$

where the estimate of the loss factor $\hat{\beta}_Q$ is given in (29). Hence, the Lyapunov function value used in the integrator reset algorithm is also an estimate. Erroneous resets due to measurement noise during estimation of z^* in (32) is reduced by decreasing the density of integrator reset candidates in $\mathcal{H}$.

H. Set-point mapping

In normal operation, increasing the rotational speed of the propeller leads to an increase in the propeller load torque. However, in case of ventilation, it might be necessary to reduce the rotational speed of the propeller in order to increase the propeller load torque, see Figure 2(b). In [5] both stationary and dynamical tests of these effects are studied. Due to the given controller design and since the desired thrust T_d is the input of the controller, a set-point mapping may prevent the controller from demanding torque above the limit of saturation:.

$$\omega^* = \begin{cases} \omega_{opt}, & \text{if } \zeta = 1 \text{ and } \omega_d \geq \omega_{opt} \\ \omega_d, & \text{otherwise} \end{cases} \tag{33}$$

where ω_{opt} is some optimal propeller speed during ventilation, $\omega_{opt}/\omega_{max} = 0.45$ in Figure 2. Further note that the ventilation detection ζ from section II-F includes hysteresis, hence robustness due to measurement noise in the loss value estimate $\hat{\beta}_Q$ is achieved.

III. Experimental test results

An experimental set-up in the Marine Cybernetics Laboratory (MCLab) at NTNU was used to test the resulting strategy. The thruster set-up had the following physical characteristics:

D	J	K_ω	K_{T0}	K_{Q0}
0.25 m	0.005 kgms^2	0.01 Nms	0.575	0.075

where the maximum speed of the propeller was $\omega_{max} = 125$ rad/s. The density of water in the basin was $\rho = 1000$ kg/m^3, and the following set of controller gains were used:

$$K_p = 0.032, \; T_i = 0.05$$

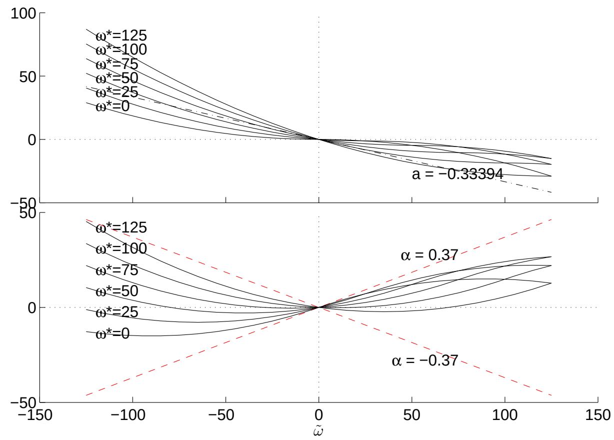

Fig. 3. **Upper:** Load torque nonlinearities $Q_p(\frac{h}{R},\omega) - Q_p(\frac{h}{R},\omega^*)$ in (12) for different values of ω^* running from $\tilde{\omega} = -125$ to $\tilde{\omega} = 125$ with $\beta_Q = 1$. The dotted line represents the linear part $-a\tilde{\omega}$ in (12). **Lower:** The minimized nonlinear term $f(\frac{h}{R},\omega^*,\tilde{\omega})$ in (12) for different values ω^* for $\tilde{\omega} \in [-125, 125]$.

In this set-up, the thruster is stationed at a fixed position, centered in the basin. Hence, the use of the nominal thrust and torque coefficients K_{T0} and K_{Q0} in (23) and (3) are appropriate.

The nonlinear term $Q_p(\frac{h}{R},\omega) - Q_p(\frac{h}{R},\omega^*)$ in (12) is shown in Figure 3 for different values of ω^*. The loss factor β_Q is assumed to be constant equivalent to 1, where the nonlinear term is most dominant.

We consider $\tilde{\omega} \in [-125, 125]$, hence $a = -0.33$ will minimize the remaining nonlinear part $f(\frac{h}{R},\omega^*,\tilde{\omega})$ enclosed inside the sector $[-\alpha, \alpha]$, see Figure 3. However, note that $f(\frac{h}{R},\omega^*,\tilde{\omega})$ is not enclosed inside the sector $[-\alpha, \alpha]$ for $|\tilde{\omega}| > 125$, but due to $\tilde{\omega} \in [-125, 125]$, exponential stability (ES) may still be ensured for all feasible initial conditions.

The resulting eigenvalues of the matrix A are $\lambda_1 = -73.4$ and $\lambda_2 = -1.7$. Including the sector $\alpha = 0.37$ from Figure 3 in Lemma 1, ES of the nonlinear function (9) is proven with $Q = \text{diag}(1, 0.1)$, $\mu_1 = 0.015$ and $\mu_2 = 0.00012$. The solution of (13) is:

$$P = \begin{bmatrix} 0.006652 & -2.5 \cdot 10^{-4} \\ -2.5 \cdot 10^{-4} & 2.1081 \end{bmatrix} \tag{34}$$

hence (15) will act as a suitable Lyapunov function.

For evaluation of the modular integrator reset strategy outlined in this paper, test scenarios are given both with and without the reset module. With reference to Figure 2, the propeller speed region of interest is selected to be located above $\omega/\omega_{max} = 0.45$. The desired thrust was therefore chosen as $T_d = 300$ N which yields $\omega_d = 73$ rad/s. Tests were performed both with and without the set-point mapping. To demonstrate extreme seas, the propeller was moved in and out of water by raising and lowering the thruster with a period of 5 seconds and an amplitude of 15 cm. The propeller was then fully submerged at its lower position, i.e. the distance from the propeller blades to the sea surface was 5 cm. In the upper position, the shaft of the propeller was in the mean free surface.

Plots of the experimental results are shown in Figure 4-7. A wave probe was used for measuring the relative

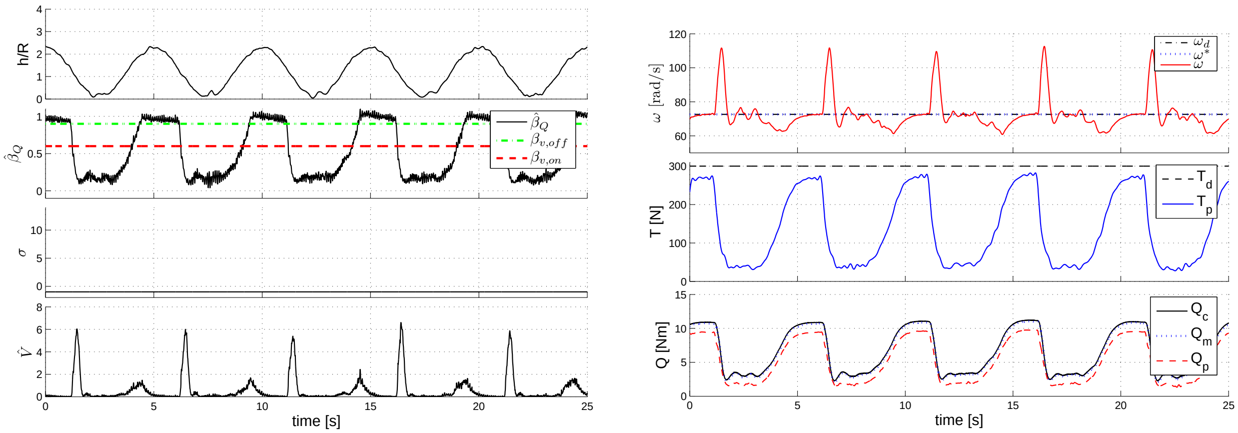

(a) (b)

Fig. 4. Experimental results with local thruster PI-control (no reset). Desired speed $\omega_d = 73$.

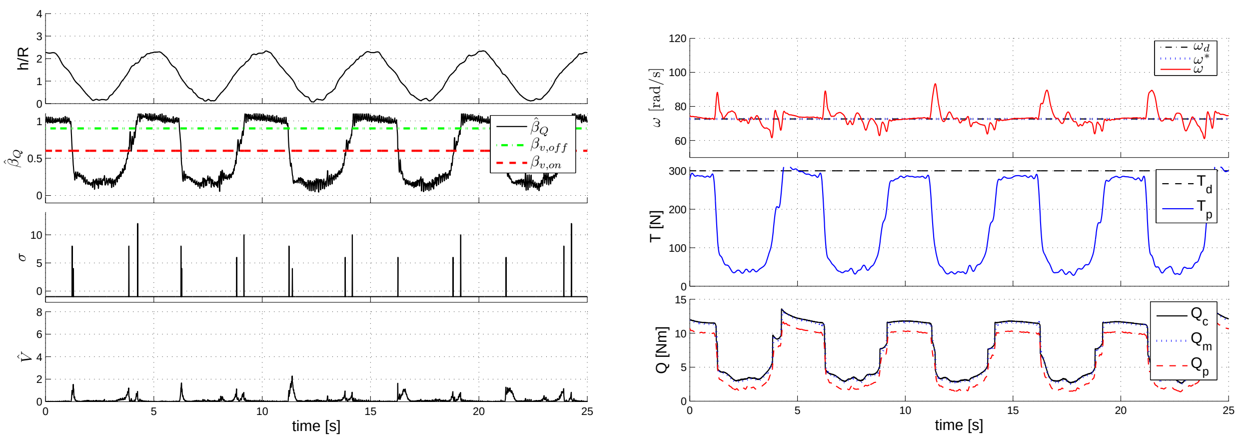

(a) (b)

Fig. 5. Experimental results of the same situation as in Figure 4, but with integrator resetting with the following candidates: $\mathcal{H} = \{0, 2, 4, 6, 8, 10, 12\}$.

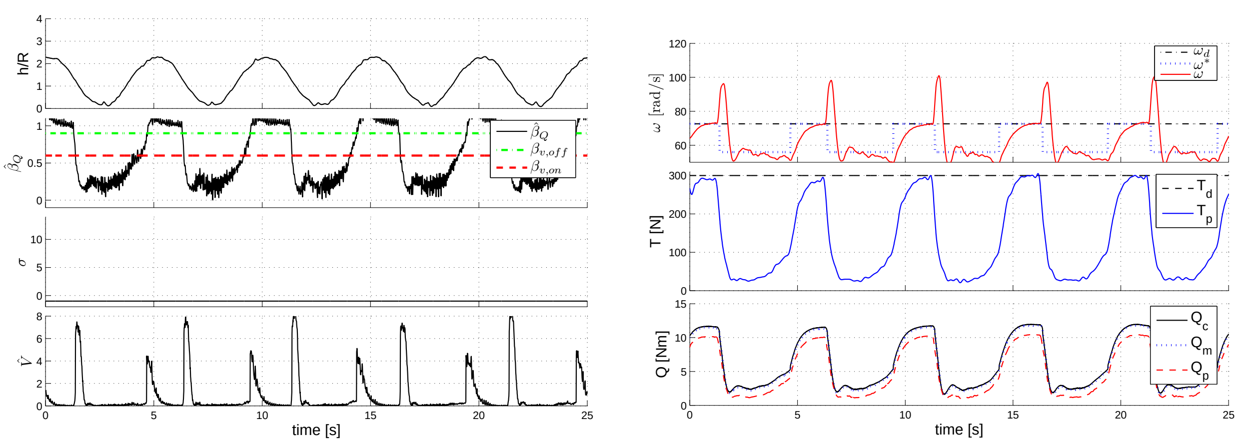

(a) (b)

Fig. 6. Experimental results with local thruster PI-control and set-point mapping (no reset). When ventilation is detected, the set-point of the PI-controller is changed from the initial $\omega_d = 73$, to a lower value $\omega^* = 56$.

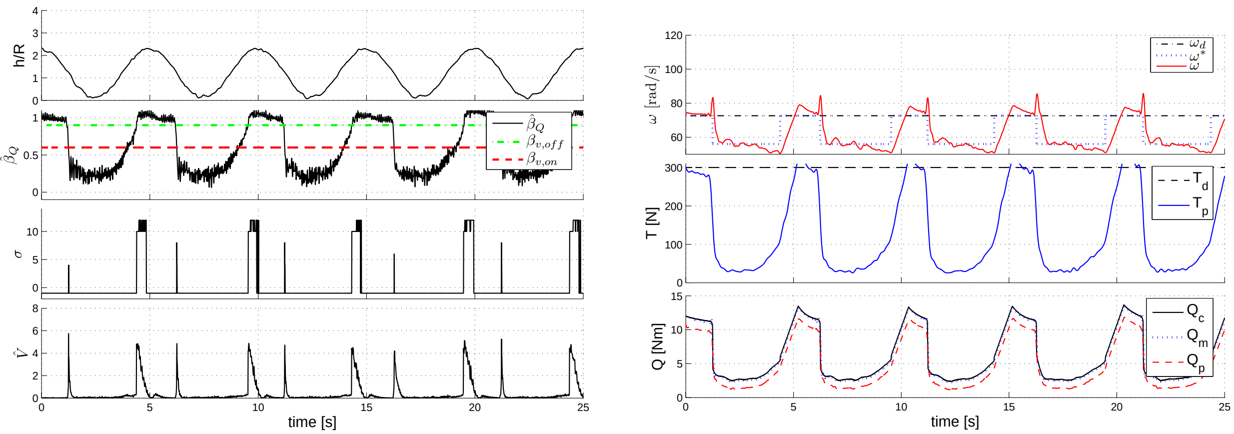

(a) (b)

Fig. 7. Experimental results of the same situation as in Figure 6, but with integrator resetting with the following candidates: $\mathcal{H} = \{0, 2, 4, 6, 8, 10, 12\}$.

submergence h/R. In order to plot the reset progress, $\sigma(t)$ is defined by:

$$\sigma = \begin{cases} z_i, & \text{if } \Delta V_i < 0 \\ -1, & \text{otherwise} \end{cases} \qquad (35)$$

The exact Lyapunov function value is not available, but an estimate $\hat{V}$ of this is included in the plots. Thrust and torque sensors on propeller shaft were used to measure T_p and Q_p. The motor time constant is neglected in this paper, supported by the likeness between commanded motor torque Q_c and measured motor torque Q_m. The discrepancy between Q_c and Q_p is mainly due to the friction K_ω.

Figure 4 shows a situation where a conventional PI-controller is used. Note the peaks in propeller speed ω when the propeller ventilates. Also note the positive jumps in the estimated Lyapunov value due to shifted equilibrium point when the propeller starts and stops ventilating. The same situation is shown in Figure 5, but with integrator resetting. Clearly, the reset leads to reduced peaks in ω. The plots of $\hat{V}$ shows the transient reductions when the PI-controller is reset. Also note that the mean propeller thrust $\bar{T}_p$ is not reduced when the PI-controller is reset: the mean propeller thrust without reset is $\bar{T}_p = 136$ N while the value with reset is $\bar{T}_p = 152$ N.

Figures 6 and 7 show the same controllers as Figures 4 and 5, but with a set-point mapping to $\omega^* = 56$ when ventilation is detected. Note the peak reduction of ω in Figure 7, where the integrator resetting is made active. In this last situation, a positive slew rate limiter has been included at the integrator output. This reduces the noise in the estimated $\hat{\beta}_Q$, and hence reduces the risk of performing erroneous resets. A more sophisticated solution to this issue would be to implement the noise reduction in the estimator $\hat{\beta}_Q$ instead. This is not considered here. A brief discussion of this problem is included in [8]. The mean propeller thrust is in this case kept more or less constant with the introduction of integrator reset: $\bar{T}_p = 130$ N without reset, while $\bar{T}_p = 128$ N with reset. The small reduction may be due to the introduction of the slew rate limiter. A more appropriate choice of this slew rate limiter may lead to an increase rather than a decrease of this value.

IV. Conclusions

We have presented a modular way of improving the transient performance of a PI-controller for marine thruster speed control by integrator resetting. A Lyapunov function is used to decide when to reset and to prove asymptotic stability of the overall system.

A test of the control strategy is made in a basin, where improved performance is observed at situations where the propeller ventilates. Tests showed reduced peaks in propeller speed, hence reduction of structural loads on propeller blades, while maintaining or even increasing the mean propeller thrust.

Acknowledgements

This work was in part sponsored by the Research Council of Norway, project number 157805/V30.

References

[1] A. J. Sørensen, "Structural Issues in the Design and Operation of Marine Control Systems," *IFAC Journal of Annual Reviews in Control*, vol. (29:1), pp. 125–149, 2005.

[2] D. Radan, Ø. N. Smogeli, A. J. Sørensen, and A. K. Ådnanes, "Operating Criteria for Design of Power Management Systems on Ships," in *Proc. of the 7th IFAC Conference on Manoeuvring and Control of Marine Craft (MCMC'06)*, Lisbon, Portugal, 2006.

[3] Ø. N. Smogeli, J. Hansen, A. J. Sørensen, and T. A. Johansen, "Anti-Spin Control for Marine Propulsion Systems," in *IEEE Conference on Decision and Control*, Bahamas, Dec. 2004.

[4] T. I. Fossen, *Marine Control Systems*, Marine Cybernetics, 1 edition, 2002.

[5] Ø. N. Smogeli, L. Aarseth, E. S. Overå, A. J. Sørensen, and K. J. Minsaas, "Anti-Spin Thruster Control in Extreme Seas," in *Proc. of the 6th IFAC Conf. on Manoeuvring and Cont. of Marine Craft (MCMC'03)*, Girona, Spain, 2003, pp. 221–226.

[6] H. K. Khalil, *Nonlinear Systems (3rd Ed.)*, Prentice-Hall, New York, 2001.

[7] M. S. Branicky, "Multiple Lyapunov Functions and Other Analysis Tools for Switched and Hybrid Systems," *IEEE Transactions on Automatic Control*, vol. (43:4), pp. 475–482, April 1998.

[8] Ø. N. Smogeli, A. J. Sørensen, and T. I. Fossen, "Design of a Hybrid Power/Torque Thruster Controller with Thrust Loss Estimation," in *Proc. IFAC Conference on Control Applications in Marine Systems (CAMS'04)*, Ancona, Italy, 2004.